IEEE Photonics Journal
An IEEE Photonics Society Publication

Open Access

Application on Minimizing Residual AM in DPSK UDWDM-PON ONU by Integrated Dual-EML

Volume 8, Number 3, June 2016

Guang Yong Chu, Member, IEEE
Iván Cano
Victor Polo
Josep Prat, Member, IEEE

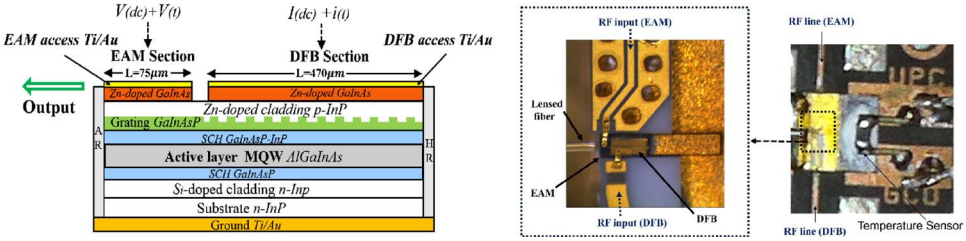

(a) (b)

DOI: 10.1109/JPHOT.2016.2566447
1943-0655 © 2016 IEEE

Application on Minimizing Residual AM in DPSK UDWDM-PON ONU by Integrated Dual-EML

Guang Yong Chu, *Member, IEEE*, Iván Cano, Victor Polo, and Josep Prat, *Member, IEEE*

Department of Signal Theory and Communications, Universitat Politècnica de Catalunya, 08034 Barcelona, Spain

DOI: 10.1109/JPHOT.2016.2566447

Manuscript received April 8, 2016; revised May 3, 2016; accepted May 6, 2016. Date of publication May 10, 2016; date of current version June 1, 2016. This work was supported by the European Information and Communication Technologies FP7 COCONUT Project under Grant GA318515, by the China Scholarship Council fellowship under Grant 201207040059, and by the Spanish Ministry of Science and Innovation FLIPER under Grant TEC2015-70835 and ROMULA under Grant TEC2011-25215. Corresponding author: G. Y. Chu (e-mail: yong@tsc.upc.edu).

Abstract: A monolithically integrated dual electroabsorption modulated laser (DEML), consisting of distributed feedback laser (DFB) and electroabsorption modulator (EAM) sections, is proposed as a transmitter in an optical network unit with phase-shift keying (PSK) modulation. The DFB is directly modulated in phase, and the EAM section is applied for mitigating the residual amplitude modulation. The DEML, as compared with external phase modulator, has advantages of low cost, simplified design, low footprint, and reasonable power consumption, thus making it attractive for an ultradense wavelength division multiplexing passive optical unit. The system is validated at 2.5 and 5 Gb/s with intradyne detection.

Index Terms: Coherent communications, fiber optics systems, optical and other properties.

1. Introduction

The explosive growth of telecommunications services has continued to fuel the deployment of optical access networks [1], [2]. Ultra-dense wavelength division multiplexing (UDWDM) with coherent detection provides a promising option for a “wavelength-to-the-user” access network [2]. However, the cost and footprint are still vital factors to be considered in customer equipment [1]–[5]. With this purpose, integrated modulators are an interesting option for transmitters (Tx), particularly at the user side.

Unlike $LiNbO_3$, monolithic integration on InP presents a lower footprint, cost, and consumption, and facilitates the design of complex photonic circuits with multiple functions [6]. In recent years, integrated chips are available for a WDM passive optical network (WDM-PON) [1]–[3], such as the semiconductor optical amplifier (SOA), reflective-SOA (RSOA) [4], [7]–[10], the binary phase shift keying electro-absorption modulated laser (BPSK-EML) [11], and the dual electro-absorption modulated laser (DEML) [11].

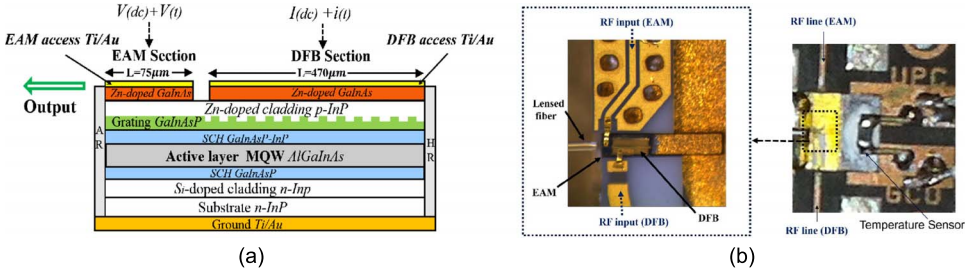

Fig. 1. (a) Side view of DEML chip structure. (b) DEML chip on a sub-mount showing RF input for DFB and EAM access ceramics.

The DEML combines a distributed feedback laser (DFB) and an electro-absorption modulator (EAM). It can be easily integrated and fabricated [11]; thus, it is attractive for Tx at the optical network unit (ONU) [3], [11], as well as the optical line terminal (OLT) [11]. Traditionally, the DEML uses the DFB as the optical carrier source and the EAM for data modulation in intensity. Unlike the traditional design on this kind of chip, the DFB can be also driven with radio frequency (RF) access, providing the capacity of modulating the DFB. In this work, the DFB section is coupled with a RF electrode for fast modulation, as well as the EAM section. Furthermore, unlike the traditional application on the DEML, a method called balanced FM-AM [11] was developed with the purpose of compensating fiber dispersion effects [11] by spectrum sculpting [12], [13]. Differently, the DFB can be directly modulated in phase by equalizing the signal [14], [15], providing a PSK modulation possibility by using the DEML. Unfortunately, there is a residual amplitude modulation (AM) caused by modulating the DFB, producing a substantial penalty in the performance [14], [16], [17]. Hence, mitigating or minimizing the residual AM is worthy of further research. Some researches present good works on reducing the residual AM [18]–[21], in this work, we focus on this new application for the DEML. Besides, for further research, this device can be useful for multi level modulation, such as quadrature phase shift keying (QPSK) and quadrature amplitude modulation (QAM) when the laser linewidth could be reduced.

For the receiver (Rx) side, coherent detection presents better performance compared with direct detection [19], [22]–[24], and it gives the benefit of wavelength selectivity for ultra-dense channel spaced network without the demand of optical filters.

We have demonstrated in [25] a 1.25 Gb/s differential phase-shift keying (DPSK) transmission by means of a DEML with a heterodyne Rx. In this work, here we extend the measurements to 2.5 Gb/s and even to 5 Gb/s using a new coherent intradyne Rx. The EAM is employed to mitigate the residual AM produced when directly phase modulating the DFB, with the technique explained in this paper. An enhancement of 2.5 dB and 4 dB for 2.5 Gb/s and 5 Gb/s are achieved when compared with a directly phase modulated DFB, showing that the residual AM is mitigated effectively.

This paper is organized as follows: In Section 2, the monolithic DEML is introduced and the characteristics are measured. The experimental setup is described in Section 3. Then, in Section 4, the mitigated residual AM effect and BER performances at 2.5 Gb/s and 5 Gb/s are shown. Finally, conclusions are presented in Section 5.

2. Monolithically Integrated DEML Assembly and Characterization

The integrated DEML is designed for temperature-stable, energy-efficient, and high-bit rate operation at an emitting wavelength of 1537 nm. The same active layer is used for both laser (DFB) and modulator (EAM) sections. The length of the DFB and EAM sections is around 470 μm and 75 μm respectively. A schematic representation of the DEML chip is shown in Fig. 1(a). The III–V epitaxial layers are grown on an InP substrate. Its intrinsic layer contains an InGaAlAs multiple-quantum well (MQW) stack sandwiched by two separate confinement

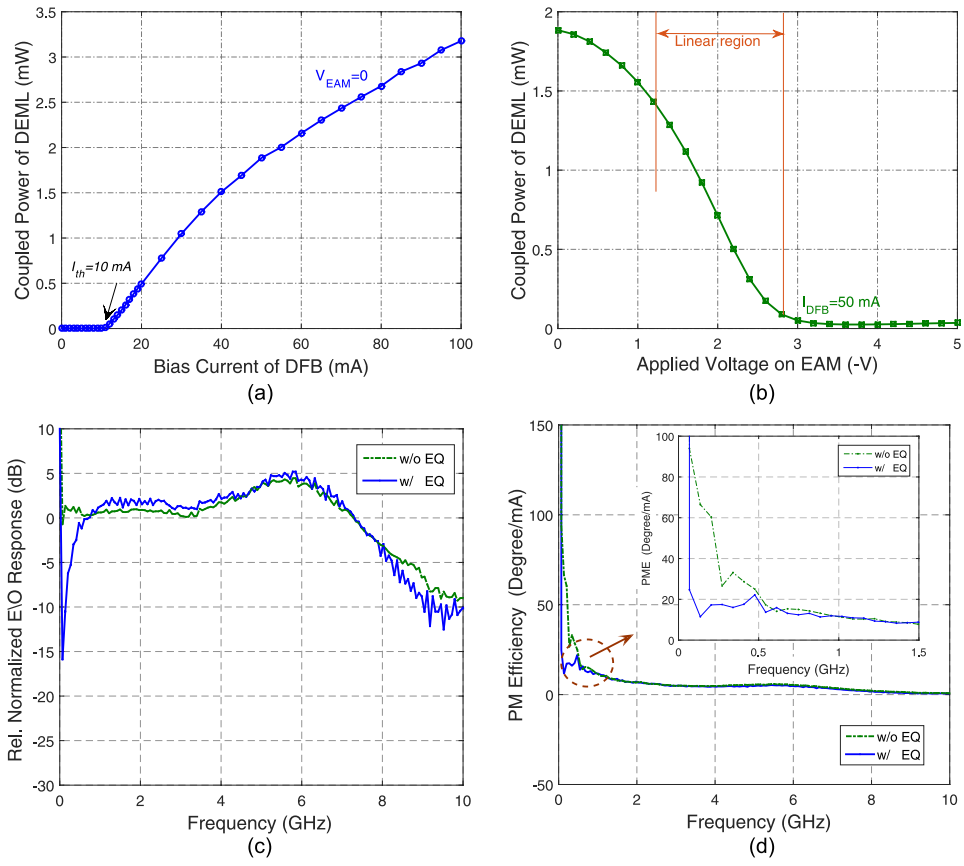

Fig. 2. (a) Characterization of the DFB of DEML. (b) Characterzation of DEML when $I_{DFB} = 50$ mA. (c) Normalized Am Responses. (d) PM efficiency in frequency domain.

heterostructures (SCH). The EAM is implemented by using a pin diode structure with the active MQW located inside the intrinsic layer [13]. The bias applied to the pin diode adjusts the electrical field in the MQW region and results in the change of optical absorption due to the quantum-confined stark effect (QCSE). In addition, the waveguide is selectively buried with a tandem layer of semi-insulating InP [11].

This assures a low EAM capacitance and low thermal resistance of the laser [13]. The DEML chip (size 0.25 mm $\times$ 0.5 mm) is on a sub-mount (size 2 mm $\times$ 6 mm $\times$ 0.5 mm) and RF data access ceramics for DFB and EAM are shown in Fig. 1(b). Both the DFB and EAM have resistors of 50 Ω for impedance matching. A microchip circuit board is used to provide the RF access to the DFB and EAM. The substrate of circuit board is RO-Duroid-5880 with 0.127 mm thickness, supporting the propriety of maximum bandwidth for the chip assembly [26].

The DFB threshold current is 10 mA as shown in Fig. 2(a). The DEML output power against the bias voltage of the EAM is plotted in Fig. 2(b). The DFB is adjusted at a bias condition of 50 mA which is a balanced value for temperature stability, maximum bandwidth, and output power. From Fig. 2(b), the bias condition of –2 V for EAM is chosen, providing around 0 dBm output power. The linewidth for the DEML is around 10 MHz. The temperature is controlled in order to avoid high wavelength drifts. The control is done by a peltier at an operating condition of 25 °C with the help of a temperature sensor.

The AM and phase modulating efficiency (PME) [27] of the DFB in this integrated DEML are obtained following the procedure described in [27]. A high pass filter based on a simple RC network equalizer is required to obtain the phase modulation [14]. The AM response and PME are shown in Fig. 2(c) and (d). It is observed that the 3-dB modulating bandwidth is around 8 GHz.

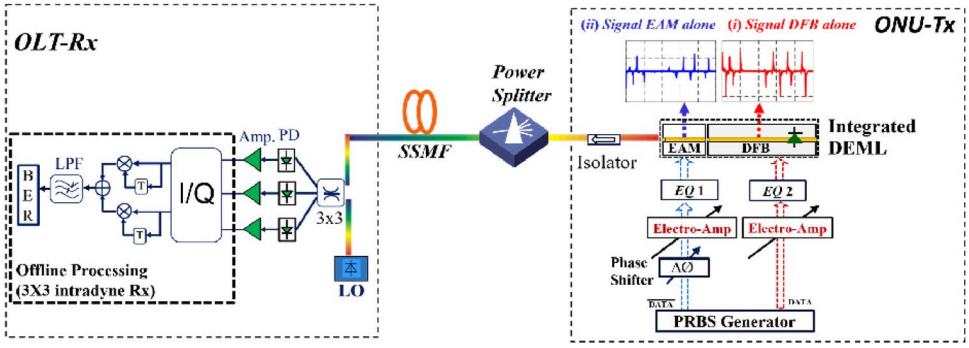

Fig. 3. DPSK with integrated DEML with coherent Rx. [Insets (i) and (ii) show the signals injecting DFB and EAM].

The PME presents a flat response at low frequencies after using the equalizer (see Fig. 2(d)), reducing phase distortions when it is modulated by the driving current.

3. Experimental Setup

The DEML is modulated with 2^{18} non-return to zero (NRZ) differentially coded bits. Data is generated to modulate both the DFB and the EAM, as shown in Fig. 3. Two electrical amplifiers are used to introduce appropriate signal power into the each device in the chip [11]. A phase shifter $(\Delta\phi)$ is used to adjust the delay of the driving signals to the DFB and EAM [11], [13].

With the purpose of modulating the DFB in phase, the data signal is equalized. Correspondingly, a second equalizer is used for providing a coordinated RF signal to the EAM. After the two equalizers, the signals are injected into the two sections of the DEML. An isolator is used for minimizing the optical reflections. After 50 km standard single mode fiber (SSMF) link, the signal is coherently detected with an intradyne Rx. The received data signal is mixed with the a local oscillator (LO) by means of a 120° optical coupler. The LO is an external cavity laser (ECL) with 0 dBm optical power [15], [28]. A polarization controller (PC) is employed for compensating fluctuations in the state of polarization (SOP) of the fiber; a polarization scrambler [28] or polarization diversity receiver could be used to avoid the PC. The coupler outputs are detected with 3 photo-diodes (PDs) followed by low noise electrical amplifiers. The electrical signals are sampled and digitally processed with a 50 GSa/s real time oscilloscope. The I and Q components are computed and filtered, and then, the samples pass through a 1-bit delay and multiply block for differential demodulation. Before bit decision, samples are low-pass filtered. Finally, the BER is computed.

4. Minimizing Residual AM of DFB via DEML

As explained in previous sections, the residual AM reduce the signal quality when modulating in phase [17], [21]. With the purpose of minimizing the residual AM, the EAM is modulated with the inverse of the data that drives the DFB. Varying the signal amplitude of the EAM can compensate the AM component of the DFB since they have opposite effects on the amplitude. For proper operation, both signals modulating the DEML are also synchronized. To guarantee this, a phase shifter $(\Delta\phi)$ is introduced as shown in Fig. 3. The effect on the BER when varying the phase shift between the DFB and EAM signals is plotted in Fig. 4(a). A phase shift of $\pm 20°$ is tolerated with less than a 1 dB penalty.

After having adjusted the delay and signal amplitude, we measure the residual AM before and after the proposed mitigation with the EAM. Fig. 4(b) shows the detected signals. The amplitude of the AM is around 315 mVpp before mitigation, whereas it is reduced by almost 40% (197 mVpp) after EAM mitigation.

Validating tests are first carried out at a bit rate of 2.5 Gb/s. The DEML is measured under the following conditions: modulating DFB alone in optical back-to-back (btb) and 50 km SMF;

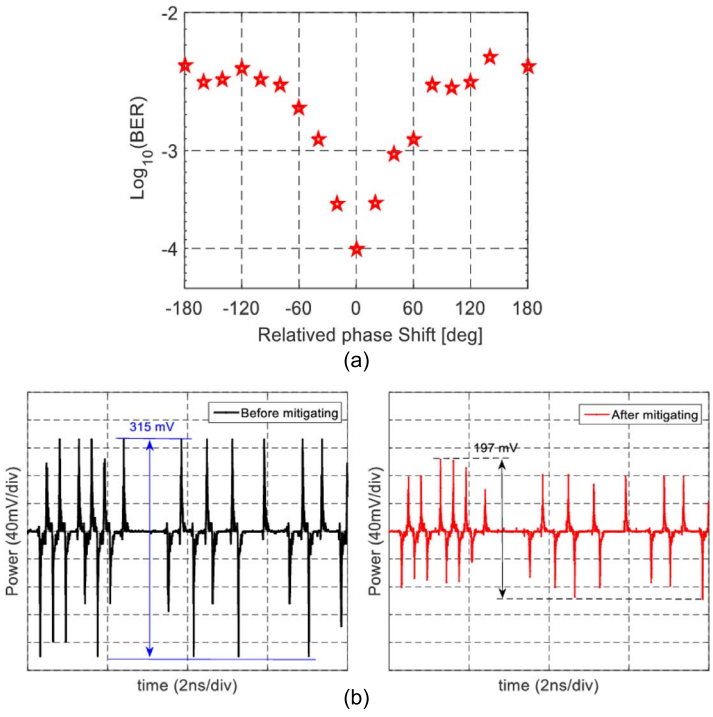

Fig. 4. (a) BER versus phase shift of the signal between DFB and EAM. (b) Detected 2.5-Gb/s signal amplitudes.

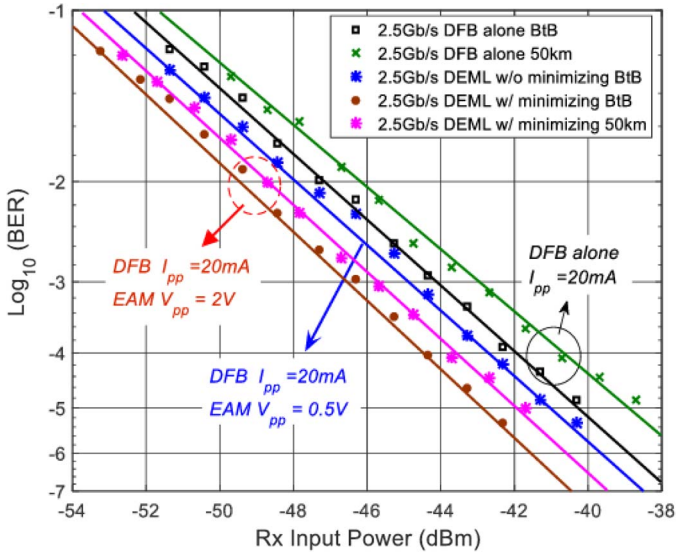

Fig. 5. BER versus Rx input power for 2.5 Gb/s.

both DFB and EAM dual driven in btb with a signal amplitude of 0.5 Vpp for the EAM; and dual driven (in btb and with 50 km SMF) with signal amplitude for EAM of 2 Vpp. For all measurements, the signal amplitude for DFB is maintained at 20 mApp. The results are shown in Fig. 5. For the DFB alone, the Rx sensitivity at BER $= 10^{-3}$, which corresponds to a 7% forward error correction (FEC) [28], [29], reaches –44 dBm and –42.9 dBm in btb and 50 km SMF, respectively. The difference between btb and 50 km SMF is mainly because of frequency drifts in the

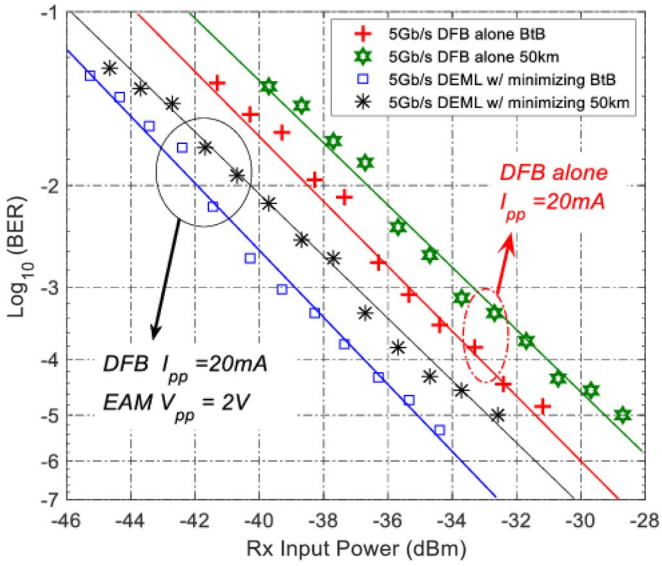

Fig. 6. BER versus Rx input power for 5 Gb/s.

Tx and LO lasers. When the EAM is used to mitigate the residual AM, the Rx sensitivity improves to –44.7 dBm in btb when the electrical signal driving the EAM is only 0.5 Vpp. The performance improvement is thus < 1 dB. However, when the EAM signal is 2 Vpp (optimum value), the Rx sensitivity reaches –46.5 dBm in btb, and –45.7 dBm with 50 km SMF. This is a 2.5 dB enhancement when compared to only modulating the DFB.

Furthermore, when we keep the DFB modulating signal at 20 mApp, varying the EAM driven voltage from 0 to 2 Vpp. The 2 Vpp presents better BER performance. Hence, we keep this condition for mitigating the residual AM.

Then, we scale the bit rate to 5 Gb/s; the EAM is driven with a 2 Vpp signal, while 20 mApp is maintained for driving DFB; it is because that the 2 Vpp for the EAM is the optimal mitigating residual AM environment. The results are shown in Fig. 6. At BER $= 10^{-3}$, the sensitivity reaches –35.3 dBm and –33.2 dBm for btb and 50 km fiber transmission respectively when modulating the DFB alone, around 2.1 dB penalty is found between btb and 50 km due to laser frequency fluctuations. When the EAM is also driven, the Rx sensitivities are –39.4 dBm, –37.5 dBm for btb and 50 km SMF correspondingly. Compared with directly modulating the DFB only, the Rx sensitivity is enhanced by 4 dB. This improvement for 5 Gb/s is higher than the one observed at 2.5 Gb/s because the residual AM is higher at 5 GHz, as can be seen in the response of Fig. 2 (c), closing to the relaxation oscillation frequency of the laser. Hence, a strong reduction of the AM noise is expected for the 5 Gb/s when driving the EAM also. In addition, a similar device with two outputs can be used as Tx and LO, further reducing the complexity of the ONU [3].

5. Conclusion

A simple form of obtaining proper PSK modulation and a cost-effective ONU Tx are demonstrated, using a novel DEML integrated device. An approach for mitigating the residual AM of integrated DEML is proposed and experimentally tested at 2.5 Gb/s and 5 Gb/s.

The synchronization between the DFB and EAM is critical, showing a tolerance of just $\pm 20^{\circ}$ for maintaining BER $= 10^{-4}$. An improvement of 2.5 dB and 4 dB on the sensitivity are obtained for 2.5 Gb/s and 5 Gb/s when the residual AM is mitigated. This can potentially help on producing multilevel formats and thus increase the bitrate. Furthermore, DEML promises an economic-efficient solution because both DFB and EAM could be easily integrated in large-scale production.

Acknowledgment

The authors wish to thank C. Kazmierski, R. Brenot, H. Debrégeas, and A. Maho from III–V Laboratory, *Nokia/Alcatel-Lucent&Thales&Leti* in France, for fruitful discussions and the DEML supply J. Giner and R. T. López from MW&RF Lab of UPC for circuit fabrication.

References

[1] Y. Luo *et al.,* "Time and wavelength division multiplexed passive optical network (TWDM-PON) for next-generation PON stage 2 (NG-PON2)," *J. Lightw. Technol.*, vol. 31, no. 4, pp. 587–593, Feb. 2013.
[2] J. Prat *et al.,* "Technologies for a cost-effective udWDM-PON," *J. Lightw. Technol.*, vol. 34, no. 2, pp. 783–791, Feb. 2016.
[3] G. Y. Chu *et al.,* "Monolithically integrated dual output DEML for full duplex DPSK-ASK and DPSK-SSB ONU in ultra-dense channel spaced access network," *J. Lightw. Technol.*, vol. 34, no. 8, pp. 2042–2048, Apr. 2016.
[4] R. Brenot, "Demystification of self-seeded WDM access," presented at the Opt. Fiber Commun. Conf., Los Angeles, CA, USA, 2015, Paper W1J1.
[5] M. Presi, R. Corsini, M. Artiglia, and E. Ciaramella, "Ultra-dense WDM-PON 6.25 GHz spaced 8 $\times$ 1 Gb/s based on a simplified coherent-detection scheme," *Opt. Exp.*, vol. 23, no. 17, Aug. 2015, Art. no. 22706.
[6] C. Kazmierski, D. Carrara, K. Lawniczuk, J. Provost, and R. Guillamet, "12.5 GB operation of a novel monolithic 1.55 m BPSK source based on prefixed optical phase switching," presented at the Opt. Fiber Commun. Conf., Anaheim, CA, USA, 2013, Paper OW4J8.
[7] G. Y. Chu *et al.,* "1.25–3.125 Gb/s per user PON with RSOA as phase modulator for statistical wavelength ONU," *Opt. Commun.*, vol. 357, pp. 34–40, Dec. 2015.
[8] G. Y. Chu, A. Lerin, I. Cano, V. Polo, and J. Prat, "Coherent ONU based on 850 μm-long cavity-RSOA for next-generation ultra-dense access network," *Chin. Opt. Lett.*, vol. 14, no. 5, May 2016, Art. no. 050605.
[9] F. Saliou *et al.,* "Self-seeded RSOAs WDM PON field trial for business and mobile front haul applications," presented at the Opt. Fiber Commun. Conf., Los Angeles, CA, USA, 2015, Paper M2A2.
[10] M. Omella *et al.,* "10 Gb/s full duplex bidirectional transmission with RSOA-based ONU using detuned optical filtering and decision feedback equalization," *Opt. Exp.*, vol. 17, pp. 5008–5013, 2009.
[11] C. Kazmierski, "Electro-absorption-based fast photonic integrated circuit sources for next network capacity scaling," *IEEE/OSA J. Opt. Commun. Netw.*, vol. 4, no. 9, pp. A8–A16, Sep. 2012.
[12] J. Binder and U. Kohn, "10 Gbits/s-dispersion optimized transmission at 1.55 μm wavelength on standard single mode fiber," *IEEE Photon. Technol. Lett.*, vol. 6, no. 4, pp. 558–560, Apr. 1994.
[13] C. Kazmierski *et al.,* "100 Gb/s operation of an AlGaInAs semi-insulating buried heterojunction EML," presented at the Opt. Fiber Commun. Conf., San Diego, CA, USA, 2009, Paper OThT7.
[14] I. N. Cano, A. Lerin, V. Polo, J. Tabares, and J. Prat, "Simple ONU transmitter based on direct-phase modulated DFB laser with heterodyne detection for udWDM-PON," presented at the Eur. Conf. Opt. Commun., London, U.K., 2013, Paper We.2.F.4.
[15] I. N. Cano, A. Lerin, V. Polo, and J. Prat, "Simplified polarization diversity heterodyne receiver for 1.25 Gb/s cost-effective udWDM-PON," presented at the Opt. Fiber Commun. Conf., San Francisco, CA, USA, 2014, Paper W4G.2.
[16] Y. C. Chung, "Recent advancement in WDM PON technology," presented at the Opt. Fiber Commun. Conf., Geneva, Switzerland, 2011, Paper Th.11.C.4.
[17] S. P. Jung, Y. Takushima, and Y. C. Chung, "Transmission of 1.25 Gb/s PSK signal generated by using RSOA in 110-km coherent WDM PON," *Opt. Exp.*, vol. 18, no. 14, pp. 14871–14877, Jul. 2010.
[18] I. N. Cano, A. Lerin, and J. Prat, "DQPSK directly phase modulated DFB for flexible coherent UDWDM-PONs," *IEEE Photon. Technol. Lett.*, vol. 28, no. 1, pp. 35–38, Jan. 2016.
[19] J. Zhang *et al.,* "11 $\times$ 5 $\times$ 9.3 Gb/s WDM-CAP-PON based on optical single-side band multi-level multi-band carrier-less amplitude and phase modulation with direct detection," *Opt. Exp.*, vol. 21, pp. 18842–18848, 2013.
[20] R. Ferreira *et al.,* "Demonstration of Nyquist UDWDM-PON with digital signal processing in real-time," presented at the Opt. Fiber Commun. Conf., Los Angeles, CA, USA, Paper Th3I.4.1.
[21] G. Y. Chu *et al.,* "Minimizing the influences of residual AM component of RSOA for DPSK UDWDM-PON," presented at the Eur. Semiconductor Laser Workshop, Paris, France, Sep. 2014, Paper SIV.3.
[22] J. Prat *et al.,* "Simple intradyne PSK system for UDWDM-PON," *Opt. Exp.*, vol. 20, no. 27, 2012, Art. no. 28758.
[23] J. M. Fabrega and J. Prat, "Homodyne receiver prototype with time-switching phase diversity and feedforward analog processing," *Opt. Lett.*, vol. 32, no. 5, pp. 463–465, Mar. 2007.
[24] J. M. Fabrega and J. Prat, "Experimental investigation of channel crosstalk in a time-switched phase diversity optical homodyne receiver," *Opt. Lett.*, vol. 34, no. 4, pp. 21350–21361, Nov. 2009.
[25] A. Lerin, G. Y. Chu, V. Polo, I. Cano, and J. Prat, "Chip integrated DFB-EAM for directly phase modulation performance improvement in UDWDM-PON," presented at the Opt. Fiber Commun. Conf., Valencia, Spain, 2015, Paper P.7.10.
[26] F. H. Wee, F. Malek, A. U. Al-Amani, and F. Ghani, "Effect of two different superstrate layers ON Bismuth Titanate (BiT) array antennas," *Sci. Rep.*, vol. 4, p. 3709, Jan. 2014.
[27] K. Sato, S. Kuwahara, and Y. Miyamoto, "Chirp characteristics of 40-Gb/s directly modulated distributed-feedback laser diodes," *J. Lightw. Technol.*, vol. 23, no. 11, pp. 3790–3797, Nov. 2005.
[28] M. Presi, M. Artiglia, and E. Ciaramella, "Electrical filter-based and low-complexity DPSK coherent optical receiver," *Opt. Lett.*, vol. 39, no. 21, pp. 6301–6303, 2014.
[29] I. N. Cano, A. Lerin, V. Polo, and J. Prat, "Polarization independent single-PD coherent ONU receiver with centralized scrambling in udWDM-PONs," presented at the Opt. Fiber Commun. Conf., Cannes, France, 2014, Paper P.7.12.